Journal of Hazardous Materials 187 (2011) 190–198

Contents lists available at ScienceDirect

Journal of Hazardous Materials

journal homepage: www.elsevier.com/locate/jhazmat

Removals of fly ash and NO in a fluidized-bed reactor with CuO/activated carbon catalysts

Jui-Yeh Rau[a], Jyh-Cherng Chen[b], Shih-Teng Huang[a], Wen-Tsung Hung[a], Ming-Yen Wey[a,*]

[a] Department of Environmental Engineering, National Chung Hsing University, Taichung 40227, Taiwan, ROC
[b] Department of Safety, Health and Environmental Engineering, Hungkuang University, Taichung 43302, Taiwan, ROC

ARTICLE INFO

Article history:
Received 30 September 2010
Received in revised form
15 December 2010
Accepted 4 January 2011
Available online 12 January 2011

Keywords:
Simultaneous removal
NO
Fly ash
Fluidized bed catalyst reactor

ABSTRACT

This study investigates the effects of fly ash compositions (SiO_2 and Al_2O_3), particle sizes (4–10 μm and 40 μm), and concentrations on the simultaneous removals of fly ash and NO using a fluidized-bed catalyst reactor. Experimental results show that the removal efficiencies of fly ash and NO at particle concentrations of 968–11,181 mg m^{-3} are 71–97% and 42–57%, respectively. SiO_2 particles have more influences than Al_2O_3 particles on the performances of fluidized-bed CuO/AC catalyst. As the concentration of fine particle increases, the pores and active sites on catalyst surface are obstructed and therefore the activities of catalysts are depressed.

1. Introduction

Acid gases (SO_2 and NO_x) and particulate matters are usually emitted from many combustion processes, such as the thermal power plants. The controls of acid gases and particular matters have been studied extensively, because they are believed to be the major causes of acid rain which is a growing threat to human health and natural environment. The concentration of fly ash produced in thermal power plants ranges from 1000 to 10,000 mg m^{-3} and the mass medium diameter (MMD) locates at 4–40 μm [1,2]. Previous studies have found that the compositions of fly ash are 43% SiO_2, 22.5% Al_2O_3, 7.7% Fe_2O_3, and 7.5% CaO [2–4]. Conventional air pollution control devices (APCDs) used for removing acid gases and fly ash from the flue gas always comprise more than two apparatuses, such as an electrostatic precipitator integrated with a wet scrubber and an NO_x converter (selective catalytic reduction with ammonia), or a semi-dry scrubber integrated with a bag filter and NO_x converter [1–3].

Several studies have shown that metal oxide catalysts (Cu, Ni, V, Fe, and Ce) based on Al_2O_3 and activated carbon (AC) can effectively remove different acid gases (SO_2 and NO_x) from the flue gas, even at low temperatures from 120 to 250 °C [5–14]. Among these catalysts, the copper catalyst has the best activity. These catalysts are attractive and important because of their particular abilities for removing different pollutants simultaneously, which can effectively reduce the investment costs and space requirements of APCDs. The ability of granular CuO/AC catalyst for removing NO and/or SO_2 has been well investigated [12–16]. The CuO/AC catalyst exhibits higher activities than conventional Cu/γ-Al_2O_3 catalyst, and the optimum content of Cu on catalyst is 3 wt.%. Overloading of CuO causes the active metals aggregated, the active sites blocked, and the consequent decrease of catalytic activity. Chemical pretreatments of AC support can increase the surface area, oxygen deposition, and acidity of catalyst. The effects of different specific surface areas, pore size distributions, acidic groups, and basic groups of AC supports on the metal dispersions and NO removal of carbon-based catalysts are also investigated [17–20].

The development of novel air pollution control technology that can remove different pollutants simultaneously has gained many attentions. Among the possible technologies, catalysis is considered to have the most potential. The catalysis/filtration system capable of simultaneously removing acid gases and particles is developing. Some studies [8,21–23] have achieved the simultaneous removals of acid gases and particles by coating sorbents/catalysts on a filter system (such as a bag or column filter). However, most of the systems are difficult to maintain the control efficiency because the catalysts are easily deactivated. The systems also undergo higher pressure drops compared to parallel passage reactors, increasing the possible attritions of filter. The fluidized-bed reactor used for filtration and catalysis has the advantages of easy continuous operation and regeneration, less plugging phenomenon caused by fly ash, higher thermal/mass transfer efficiency, higher gas/solid or

* Corresponding author. Tel.: +886 4 22852455; fax: +886 4 22862587.
E-mail address: mywey@dragon.nchu.edu.tw (M.-Y. Wey).

0304-3894/$ – see front matter © 2011 Elsevier B.V. All rights reserved.
doi:10.1016/j.jhazmat.2011.01.018

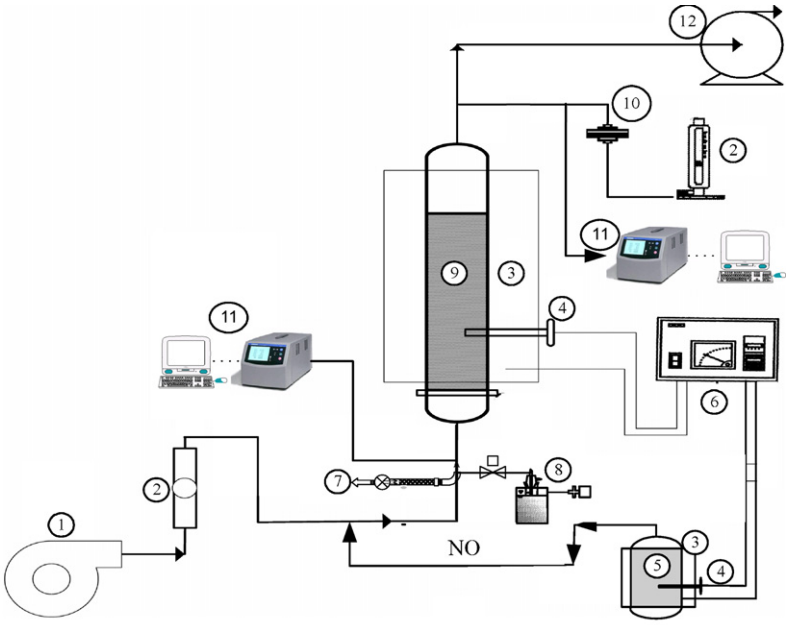

① Blower; ② Flow meter; ③ Heating system; ④ Thermocouple; ⑤ Primary combustion system; ⑥ PID controller; ⑦ Particle feeder; ⑧ NH_3 feeder; ⑨ Fluidized-bed catalyst reactor; ⑩ Particle sampling train; ⑪ Flue gas online analyzer; ⑫ Induced fan

Fig. 1. Schematic of experimental apparatus.

solid/solid contact efficiency, higher tolerance to variations in gas flow rate, and easy to replace or replenish the catalysts [24–27]. Moreover, the filtration of fly ash using a fluidized bed reactor has been well examined in our previous studies [1–4]. The results indicate that the optimum condition for fly ash filtration occurs at the ratio of operating fluidization velocity/minimum fluidization velocity (U_o/U_{mf}) lower than 2.5. In addition, the attrition of the bed materials is not apparent during the filtration of fly ash.

This study combines the advantages of fluidized-bed filtration and catalysis to develop the fluidized-bed catalyst reactor for simultaneous removals of NO and fly ash. The effects of different concentrations and sizes of fly ash on the performance of fluidized-bed catalyst reactor are investigated. The simulated flue gas contains NO gas and different compositions (Al_2O_3 and SiO_2), concentrations (~1000 and ~10,000 mg m^{-3}), and particle sizes (fine: 4–10 μm; coarse: 40 μm) of fly ash. The removal efficiencies of fly ash and NO, as well as the particle size distribution (PSD) are measured. The surface characters, physical texture, and crystal species of catalysts are also investigated.

2. Experimental

2.1. Preparation of catalysts

Activated carbon (AC) has been well demonstrated to have excellent physical and chemical properties for catalyst support [12–15]. In this study, the commercial AC used for catalyst support was classified as a Geldat B powder and purchased from China Activated Carbon Industries Ltd. in Taiwan. The AC support was sieved into particles with diameters between 16 and 20 mesh, and pretreated with 36 vol.% HNO_3 for 48 h at room temperature (designated as AC-N). The AC support pretreated with 36 vol.% HNO_3 can modify the porous structures and surface functional groups, increase the Brønsted acidity, and improve the dispersion of active metals on AC surface. After acid treatment, the modified AC-N was washed with distilled water and air-dried for 24 h at 110 °C. The active metal of CuO/AC-N catalyst was loaded by pore volume impregnation method. The AC-N supports (BET surface area of 1044.1 m^2 g^{-1}) were impregnated with copper(II) nitrate solution. After impregnation and drying at 110 °C for 24 h, the catalysts were calcined at 400 °C for 4 h. The content of Cu on CuO/AC-N catalysts was 3.0 wt.%, which was confirmed by ICP analysis.

2.2. Experimental apparatus and procedure

A laboratory-scale fluidized bed catalytic reaction system was set up, as illustrated in Fig. 1. The reaction system included a NO generation unit, a fly ash feeding unit, a fluidized-bed catalyst reactor (with 5.5 cm inner diameter and 120 cm height), and the pollutant analysis system. NO gas was generated from the combustion of artificial feedstock containing urea powder and packing paper, and the fly ash was fed with commercial Al_2O_3 or SiO_2 particles. Because SiO_2 and Al_2O_3 are the major components of fly ash in a wall-fired power plant, commercial SiO_2 and Al_2O_3 particles were used to simulate the fly ash and study the influences of different compositions on particle filtration. The mean diameters of commercial SiO_2 and Al_2O_3 particles were approximately 4–10 μm and 40 μm. The pictures of field emission scanning electron microscopy (FESEM) and particle size distribution (PSD) for the commercial SiO_2 and Al_2O_3 particles are shown in Fig. 2. In addition, the artificial feedstock was subjected to elemental analysis. The elemental compositions of packing paper and urea powder were C: 41.25%, H: 7.18%, O: 50.03% and N: 47.68%, C: 20.17%, H: 6.84%, O: 0.49%, respectively.

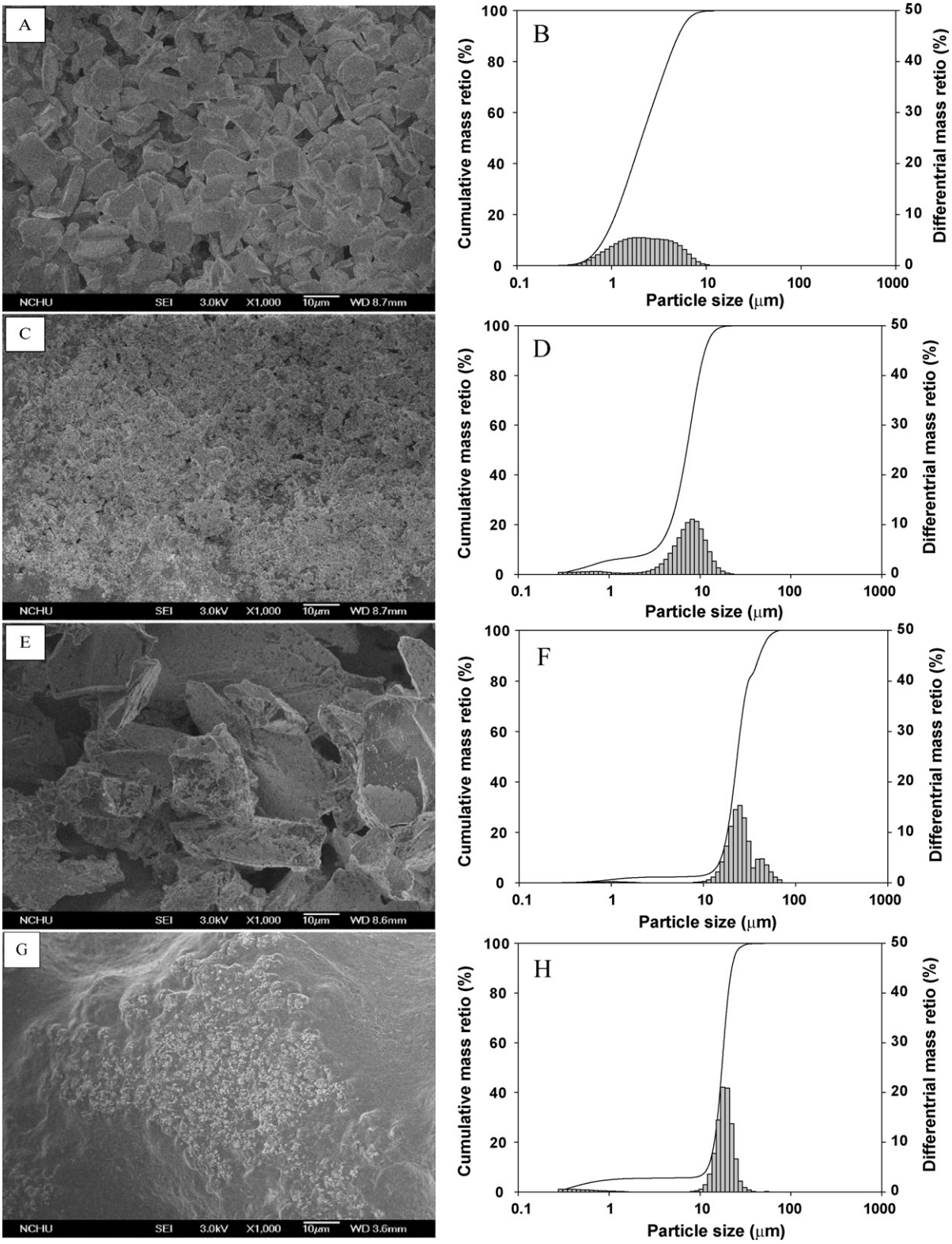

Fig. 2. FESEM images and particle size distribution of 4–10 μm (A and B: Al_2O_3; C and D: SiO_2) and 40 μm (E and F: Al_2O_3; G and H: SiO_2) particles.

Prior to the formal experiments, the combustion chamber was electrically heated to 700 °C and the input air flow rate was controlled at 45 L min^{-1}. As the combustion temperature reached a steady state, the artificial feedstock containing urea powder and packing paper was semi-continuously fed into the combustor at a regular interval of 20 s. Sampling tasks were carried out when the whole system reached a steady state. The sampling time was 3 min. The removal efficiency of particles and NO is defined as follows:

$$\text{Removal efficiency}\,(\%) = \frac{C_o - C_f}{C_o} \times 100 \quad (1)$$

Table 1
Experimental conditions of fluidized-bed catalyst reactor.

Catalyst	3% CuO/AC-N	Weight	89 g
AC density	1.36 g cm^{-3}	AC size	840–1190 μm
Reactor dimension	I.S.: 5.5 cm	Height	120 cm
Static height of catalysts	8 cm		
Reaction temp.	250 °C		
Gas velocity (U_o)	0.28 m s^{-1}		
Minimum fluidization velocity (U_{mf})	0.19 m s^{-1}	U_o/U_{mf}	1.47
Reaction time	40 min		

Table 2
Experimental conditions of NO-producing and particle feeding system.

NO-producing system			
Combustion temp.	700 °C	Flow rate	45 L min^{-1}
Combustion of artificial waste	Urea powder		
Feed rate of urea powder	12 g min^{-1}		
Conc. of input NO	426.6 ± 67.6 ppm		
Conc. of input O_2	4.2–6.3%		
Particle feeding system			
Composition of particle	SiO_2 and Al_2O_3		
Particle size	4–10 μm and 40 μm		
Conc. of input particle	1067 ± 87 mg m^{-3} (~1.8 mg min^{-1}) and 10,277 ± 1185 mg m^{-3} (~18 mg min^{-1})		
Run time	40 min		

where C_o and C_f are the inlet and outlet concentrations of the pollutants, respectively. Tables 1 and 2 summarize the major operation parameters in the experiments.

Because some catalysts may be elutriated from the fluidized-bed reactor and which would influence the exact amounts of particles passing through the fluidized-bed reactor, the elutriation tests must be carried out to determine the mass of elutriated particles from the catalysts. The detailed elutriation procedures have been described in our previous studies [1–3,28]. The mass of elutriated bed materials must be subtracted from the total mass of output particles to yield the exact concentrations of output particles. Prior to each experiment, the inner wall of fluidized-bed reactor and the ducts were cleaned carefully to avoid the interferences. After the elutriation test, the filtration experiment was performed without replacing the catalyst.

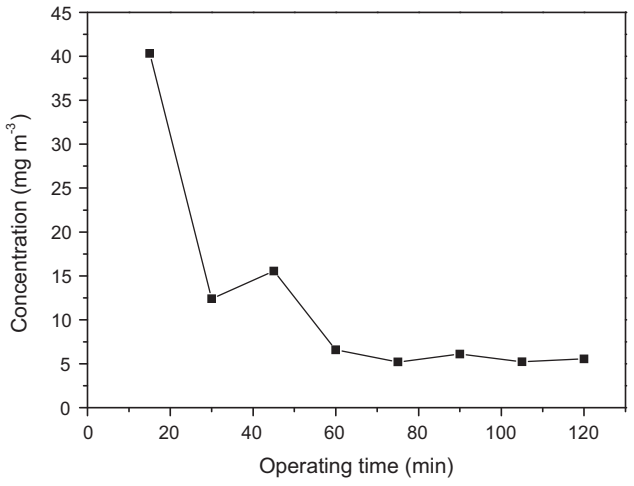

Fig. 3. Results of elutriation test for the fluidized-bed catalyst reactor at 250 °C.

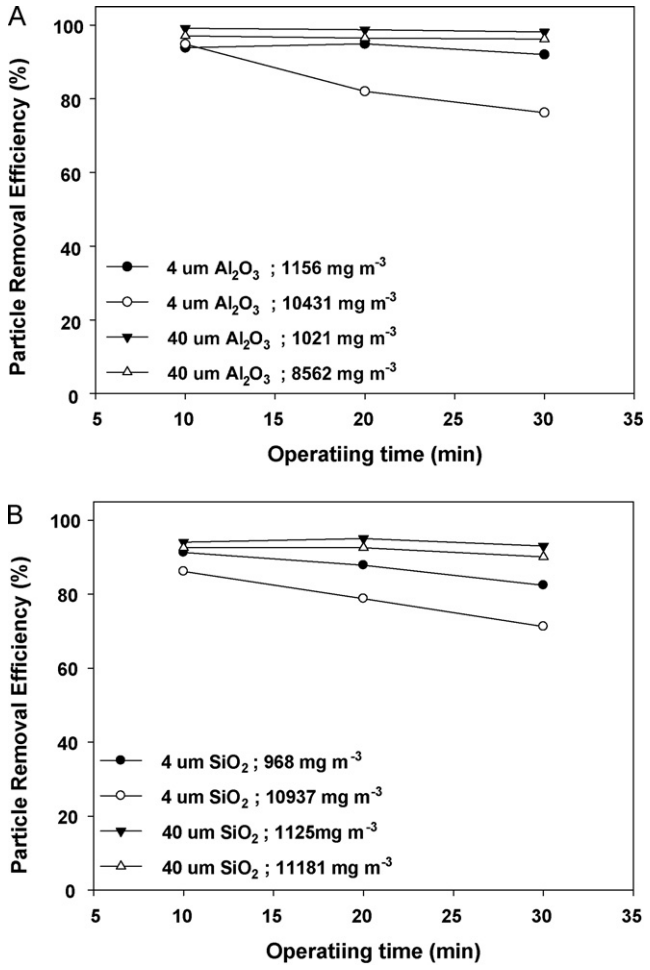

Fig. 4. Removal efficiencies of different fly ash compositions (A: Al_2O_3 and B: SiO_2) by the fluidized-bed catalyst reactor at 250 °C.

2.3. Sampling and analysis

2.3.1. NO concentration

The concentrations of O_2 and NO were measured continuously in the inflow and outflow of fluidized bed catalyst reactor. To monitor the gas concentrations, a flue gas analyzer (Horiba, PG-250) with a chemiluminescence (cross-flow modulation) sensor for NO measurement and a galvanic cell sensor for O_2 measurement was used. The analyzer was connected to a laptop to record data via RS-232C interface. Before analysis, a five-point calibration and a zero check were performed with the standard gases.

2.3.2. Characterization of CuO/AC-N catalyst

Several techniques were carried out to characterize the catalysts. An X-ray powder diffractometer (XRPD), equipped with a Cu tube as the X-ray source (MAC Science, MXP 18), was used to identify the crystalline species on catalysts. The scanning range and

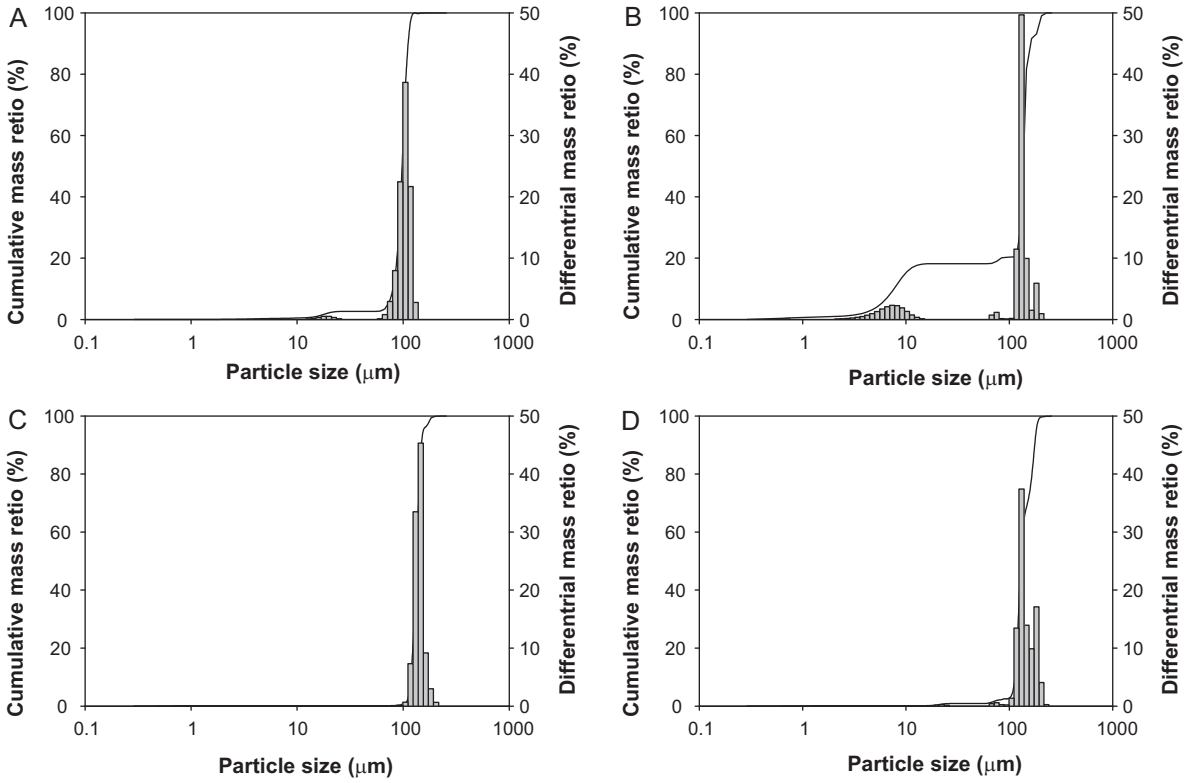

Fig. 5. Particle size distributions of eluding Al_2O_3 (A: 4–10 μm; 10,431 mg m^{-3} and C: 40 μm; 8562 mg m^{-3}) and SiO_2 (B: 4–10 μm; 10,937 mg m^{-3} and D: 40 μm; 11,181 mg m^{-3}) particles in the exhaust gas at 250 °C.

speed of XRPD were controlled at the 2θ of 20–60° in steps of 0.04° and 1.5° min^{-1}, respectively. The morphologies of the catalysts were observed using a FESEM (Model JSM-6700F, JEOL, Tokyo, Japan) which was operated with an accelerating voltage of 3 kV. The surface areas of AC support and catalyst were measured by a vacuum microbalance (BET-201-AEL, Porous Materials Inc., New York, USA) using gravimetric methods at 77 K. The surface areas of catalysts were measured from N_2 adsorption and desorption isotherms using the BET method.

3. Results and discussion

3.1. Removal efficiencies of different fly ash components

Prior to the formal experiments, the elutriation tests were carried out to determine the amounts of catalyst elutriated from the fluidized-bed reactor. The elutriated catalysts are all captured in a back filter and the amounts of elutriated catalysts depends on the operating time, the dynamic concentrations of elutriated catalysts in the flue gas can be determined from the weight differences of the filter. Fig. 3 shows the concentrations of elutriated catalysts at different operating times. The results indicate that the elutriation rates and attrition rates of catalysts are mitigated with the increase in operating time. During the fluidization of catalysts, the elutriated particles are notably smaller than those remaining in the bed.

After the elutriation test, the formal experiments were carried out without replacing the catalysts. Fig. 4 shows the removal efficiencies of Al_2O_3 and SiO_2 with different sizes and concentrations. The weights of elutriated catalyst and the remaining particles on the distributor and duct were subtracted from the input weights to determine the exact removal efficiencies of Al_2O_3 and SiO_2 by the fluidized-bed reactor. In the case of low-concentration Al_2O_3 filtration, the removal efficiency of 40 μm Al_2O_3 maintains at 99–98%, and the removal efficiency of 4–10 μm Al_2O_3 is 92–94%. In the case of high-concentration Al_2O_3filtration, the removal efficiency of 40 μm Al_2O_3 maintains at 97–96%; however, the removal efficiency of 4–10 μm Al_2O_3 falls from 94% to 76% with the operating time increased.

For both the cases of low- and high-concentration SiO_2 filtrations, the removal efficiency of 40 μm SiO_2 maintains at 95–90%, whereas the removal efficiency of 4–10 μm SiO_2 falls from 91% to 82% and 86 to 71% for low and high concentrations, respectively. These results indicate that the removal efficiencies of fly ash are decreased at the conditions of high concentrations and fine particles (Al_2O_3 and SiO_2). Moreover, the removal efficiency of Al_2O_3 particle is higher than those of SiO_2 particle. This phenomenon is attributed to the higher density of Al_2O_3 particle than SiO_2. Particles with higher density are more effectively captured by the fluidized bed catalysts through the inertial impact mechanism.

Fig. 5 displays the PSD of eluding SiO_2 and Al_2O_3 particles in the exhaust gas at 250 °C. Fig. 5(A) shows the PSD of eluding Al_2O_3 particles in the case of fine (4–10 μm) Al_2O_3 particle filtration. Two peaks of particle size distribution are located at 19 μm and 105 μm, and the mass percentages are 2.5% and 73%, respectively. For the coarse Al_2O_3 particle filtration (Fig. 5(C)), the PSD of eluding Al_2O_3 particles is mono-dispersion. The peak of particle size distribution is located at 146 μm and the mass percentage is 87%.

Fig. 5(B) and (D) plots the PSD of eluding SiO_2 particles in the cases of fine and coarse SiO_2 particle filtrations. For fine SiO_2 particle (4–10 μm) filtration, the PSD of eluding SiO_2 particles has two peaks at 8 μm and 131 μm and the mass percentages are 13% and 81%, respectively. For coarse SiO_2 particle (40 μm) filtration, the PSD is mono-dispersion with a peak at 146 μm and the mass percentage is 78%.

Above results indicate that the PSD of eluding particles moves to bigger sizes when the size of input particle increases. The coarse particles (40 μm) are well captured in the fluidized-bed reactor, and the removal efficiency is much higher than those of fine particles

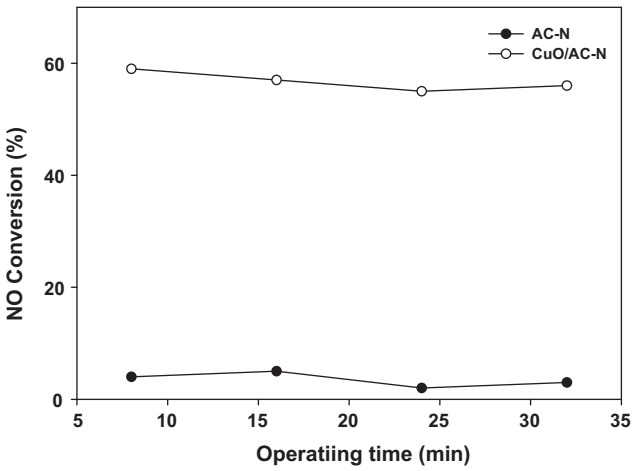

Fig. 6. Conversion efficiencies of NO by the AC-N support and CuO/AC-N catalysts in the fluidized-bed reactor.

(4–10 μm). Moreover, the results also indicate that the Al_2O_3 and SiO_2 particles are harder than the CuO/AC-N catalyst and they are less abraded in the fluidized bed.

3.2. Effects of ash content on the removal of NO

Fig. 6 shows the NO conversion efficiencies of AC-N support and fluidized-bed CuO/AC-N catalyst reactor at 250 °C. The inlet flue gas contains 410.7 ± 81.4 ppm NO, 4.2–6.3% O_2, and NH_3/N = 1–2. In the case of AC-N support (without active metals), the NO conversion efficiency is only 2–5%. The AC-N supports have very low activity on NO conversion. On the other hand, the NO conversion efficiency of CuO/AC-N catalysts increases to 55–59%.

The effects of particle sizes and concentrations on NO removal by the fluidized-bed CuO/AC-N catalyst reactor are shown in Fig. 7. The inlet flue gas contains 488.5 ± 97.4 ppm NO, 4.2–6.3% O_2, and NH_3/N = 1–2 at 250 °C. In Fig. 7(A), the NO conversion efficiency of fluidized-bed catalysts is 57–53% and 57–55% for the cases of adding low-concentration 4–10 μm and 40 μm Al_2O_3 particles, respectively. As the input particle concentrations increase from 8562 to 10,431 mg m^{-3}, the NO conversion efficiency decreases from 55% to 50%. Fig. 7(B) shows the NO conversion efficiencies of CuO/AC-N catalysts with different SiO_2 particle sizes and concentrations at 250 °C. The conversion efficiencies of NO in the cases of adding 968 mg m^{-3} (4–10 μm) SiO_2, 1125 mg m^{-3} (40 μm) SiO_2, and 11,181 mg m^{-3} (40 μm) SiO_2 are 55–49%, 54–51%, and 55–49%, respectively. The conversion efficiency of NO is decreased when the concentration of 4–10 μm SiO_2 particles rises to 10,937 mg m^{-3}.

The presences of different fly ash constituents (Al_2O_3 and SiO_2) and particle sizes (4–10 μm and 40 μm) inhibit the activity of CuO/AC-N catalyst. The inhibition effect is related to the increase of particle concentration. Because Al_2O_3 and SiO_2 particles have higher densities and hardness than CuO/AC-N catalysts, the strong impacts and accumulations on the surface of fluidized-bed catalysts are significant [1–3]. In addition, fine particles (4–10 μm) can cover or block the surface of catalyst. These phenomena are all destructive to the activity of catalyst.

3.3. Characterization of catalysts

3.3.1. Surface microstructures of fresh and spent catalysts

Fig. 8 shows the surface morphologies of fresh and spent catalysts. Fig. 8(A) displays the surface of AC-N support, and Fig. 8(B) shows CuO particles well dispersed on the surface of AC support. The particle size of Cu is approximately 40–60 nm. The species of

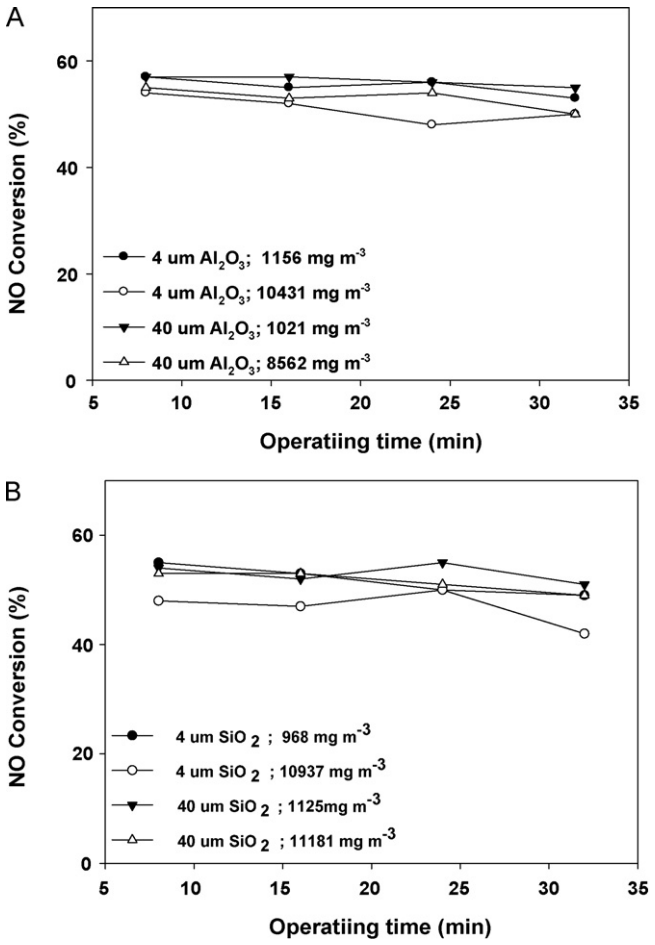

Fig. 7. Effects of particle sizes and concentrations (A: Al_2O_3 and B: SiO_2) on NO removals by the fluidized-bed catalyst reactor.

oxidization and acid treatments on the support could interact with adsorbed water to form Brönsted acid sites on the AC surface during the coating process, which may promote the dispersion of CuO [13–15]. For the spent catalysts, Fig. 8(C) and (E) shows that the aggregation phenomenon of particles on the surface of CuO/AC-N catalysts is not significant during the filtration of low- and high-concentration 4–10 μm Al_2O_3 particles. In contrast, the aggregation of fine SiO_2 particles can be observed in Fig. 8(D) and (F). When the concentration of fine SiO_2 particle increases, the aggregation phenomenon becomes more significant. In addition, Fig. 8(G)–(J) shows that Al_2O_3 and SiO_2 particles are not aggregated on the surface of CuO/AC-N catalyst. Some filtration studies [1–3,29,30] have indicated that the filtered particles may accumulate on or inset into the surface of fluidized bed media. The results are caused by the strong inertial impacts and interceptions of particles on the surface of fluidized bed granular media [1,2,31,32]. The increase of particle concentration may result in higher contact efficiency between particles and inter-particle forces. These phenomena lead to higher filtration efficiency of fly ash. However, these points are also the possible reasons to decrease the conversion efficiency of NO in the fluidized-bed CuO/AC-N catalyst reactor.

3.3.2. XRPD analysis of fresh and spent catalysts

XRPD analysis can determine the crystal species on fresh and spent CuO/AC-N catalysts. As shown in Fig. 9(A), two broad diffraction peaks are observed at $2\theta = \sim 25^\circ$ (amorphous shape) and $\sim 45^\circ$ (graphitic shape, 1 1 1) for all catalysts. The result indicates that the AC-N support has low graphitization degree. Moreover, the

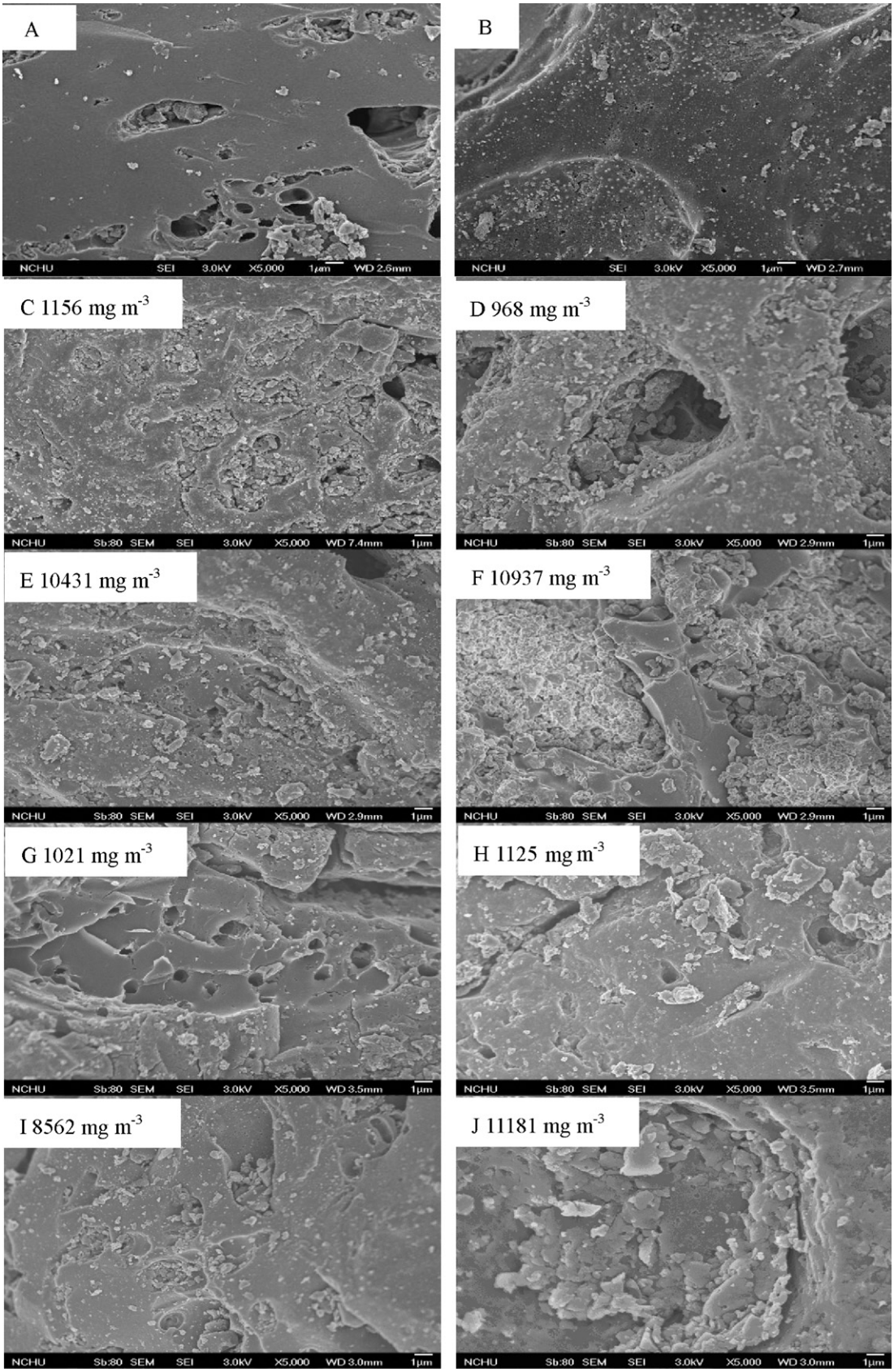

Fig. 8. FESEM images of fresh (A: AC-N; B: CuO/AC-N) and spent CuO/AC-N catalysts after the filtrations of 4–10 μm Al_2O_3 (C and E), 40 μm Al_2O_3 (G and I), 4–10 μm SiO_2 (D and F), and 40 μm SiO_2 (H and J).

Table 3
Surface characteristics of fresh and spent CuO/AC-N catalysts.

Samples	BET area ($m^2\ g^{-1}$)	V_{micro} (%)	V_{meso} (%)	V_{macro} (%)	V_{total} ($cm^3\ g^{-1}$)
Fresh catalyst					
CuO/AC-N	1044.1	81.6	17.3	1.1	0.5957
Spent catalysts					
Without particle filtration	1159.4	82.8	16.6	0.6	0.6477
For SiO_2 filtration					
4–10 μm (968 mg m^{-3})	979.8	84.4	14.8	0.8	0.5469
4–10 μm (10,937 mg m^{-3})	910.4	86.6	12.6	0.8	0.4814
40 μm (1125 mg m^{-3})	1076.1	83.9	15.3	0.8	0.6026
40 μm (11,181 mg m^{-3})	1058.8	84.4	14.9	0.7	0.5807
For Al_2O_3 filtration					
4–10 μm (1156 mg m^{-3})	1081.4	84.3	14.9	0.8	0.6008
4–10 μm (10,431 mg m^{-3})	1081.8	83.6	15.6	0.8	0.5808
40 μm (1021 mg m^{-3})	1115.9	83.0	15.9	1.1	0.6241
40 μm (8562 mg m^{-3})	1103.1	84.5	14.7	0.8	0.5937

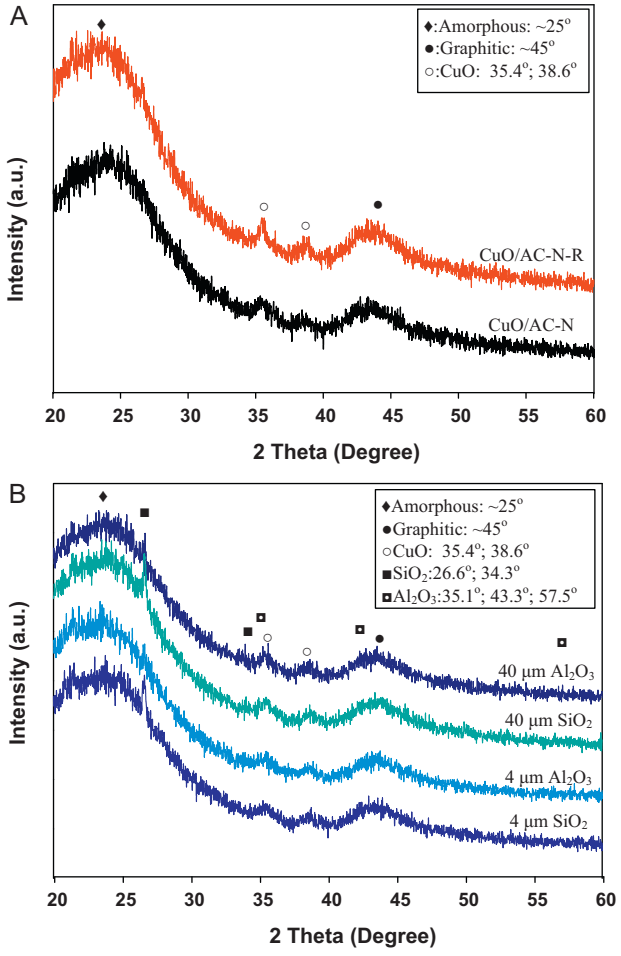

Fig. 9. XRPD patterns of fresh (A) and spent (B) CuO/AC-N catalysts (at particle concentration of 10,277 ± 1185 mg m^{-3}).

existence of CuO species is consistent with the Joint Committee of Powder Diffraction Standards (JCPDS) cards [33]. For fresh and spent CuO/AC-N catalysts, the diffraction peaks of CuO are observed at $2\theta = 35.4^\circ$ (0 0 2) and 38.6° (1 1 1) [34]. In the case of spent CuO/AC-N catalysts shown in Fig. 9(B), the major peaks of CuO ($2\theta = 35.4^\circ$ and 38.6°) can be observed. In addition, the peak of SiO_2 ($2\theta = 26.6^\circ$) is present after the filtration of high-concentration SiO_2 particles. This is also consistent with the FESEM results. Furthermore, Fig. 9(B) displays some catalysts without any clear diffraction peaks of Al_2O_3 (35.1°, 43.3°, and 57.5°) and SiO_2 (34.3°). This implies that either the concentration of particles (SiO_2 and Al_2O_3) is inferior to the detection limits or the particles are well dispersed on CuO/AC-N catalyst. Related studies [35,36] have shown that the intensity of diffraction peak was reduced because of either a lower metal loading (<5%) or a good dispersion on the support surface.

3.3.3. BET analysis of fresh and spent catalysts

Table 3 presents a summary of the surface characteristics of fresh and spent catalysts. The surface area, V_{micro}, V_{meso}, and V_{macro} of fresh and spent CuO/AC-N catalysts are 1044.1 $m^2\ g^{-1}$, 81.6%, 17.3%, 1.1%, and 1159.4 $m^2\ g^{-1}$, 82.8%, 16.6%, 0.6%, respectively. In the case of 4–10 μm SiO_2 filtration, the surface areas of catalysts at the particle concentrations of 968 and 10,937 mg m^{-3} are 979.8 and 910.4 $m^2\ g^{-1}$, respectively. The surface areas of spent/fresh CuO/AC-N catalysts at these two conditions decrease by 6.2% and 12.8%. The total pore volumes of catalysts at the particle concentrations of 968 and 10,937 mg m^{-3} are 0.5469 and 0.4814 $cm^3\ g^{-1}$, respectively. The total pore volumes of spent/fresh CuO/AC-N catalysts at these two conditions decrease by 8.2% and 19.2%. In the other cases of Al_2O_3 (fine and coarse) and SiO_2 (coarse) particle filtrations, the surface areas and pore volumes of catalysts do not have any significant change. However, the fine SiO_2 particles obstruct the pore volume of catalyst, and this obstruction effect increases with the rising concentration of particles.

4. Conclusions

The simultaneous removal efficiency of NO and fly ash by a fluidized-bed CuO/AC-N catalyst reactor is studied. The effects of different particle compositions (SiO_2 and Al_2O_3), particle sizes and concentrations are also investigated. The fly ash inhibits the activity of catalyst and the inhibition effect increases with the concentration of fly ash. The simultaneous removal efficiencies of particles and NO with the particle concentrations of 968–11,181 mg m^{-3} maintain at 97–71% and 57–42%, respectively. The poisons of catalyst by fly ash are much related to the fine and high-concentration particles in the flue gas. Several experimental techniques (FESEM, XRPD, PSD and BET) are used to characterize the fresh and spent catalysts. The PSD results show that the fine particles of SiO_2 will integrate to form coarse particles in the fluidized-bed catalyst reactor. In particular, the BET results show that the increased concentrations of fine SiO_2 particles obstruct the pore volume of catalyst. This aggregation phenomenon on the catalyst surface leads to the decrease in NO conversion efficiency. Finally, the results of this study demonstrate that the fluidized-bed catalyst reactor is highly potential for the simultaneous removals of NO and fly ash, especially for the flue gas with high concentration of particles.

Acknowledgement

The authors would like to thank the National Science Council of the Republic of China, Taiwan for financially supporting this research under Contract No. NSC 97-2221-E-005-044-MY3.

References

[1] K.Y. Liu, J.Y. Rau, M.Y. Wey, The collection of SiO_2, Al_2O_3 and Fe_2O_3 particles using a gas–solid fluidized bed, J. Hazard. Mater. 171 (2009) 102–110.
[2] K.Y. Liu, M.Y. Wey, Filtration of fly ash using fluidized bed at 300–500 °C, Fuel (2007) 161–168.
[3] K.Y. Liu, M.Y. Wey, Filtration of nano particle by a gas–solid fluidized bed, J. Hazard. Mater. 147 (2007) 618–624.
[4] M.Y. Wey, K.H. Chen, K.Y. Liu, The effect of ash and filter media characteristics on particle filtration efficiency in fluidized bed, J. Hazard. Mater. B121 (2005) 175–181.
[5] Y. Wang, Z. Liu, L. Zhan, Z. Huang, Q. Liu, J. Ma, Performance of an activate carbon honeycomb supported V_2O_5 catalyst in simultaneous SO_2 and NO removal, Chem. Eng. Sci. 59 (2004) 5283–5290.
[6] S. Sumathi, S. Bhatia, K.T. Lee, A.R. Mohamed, Selection of best impregnated palm shell activated carbon (PSAC) for simultaneous removal of SO_2 and NO_x, J. Hazard. Mater. 176 (2010) 1093–1096.
[7] Y.A. Kim, J.H. Choi, J. Scott, K. Chiang, R. Amal, Preparation of high porous Pt–V_2O_5–WO_3/TiO_2/SiC filter for simultaneous removal of NO and particulates, Powder Technol. 180 (2008) 79–85.
[8] S. Nacken, S. Heidenreich, M. Hackel, G. Schaub, Catalytic activation of ceramic filter elements for combined particle separation, NO_x removal and VOC total oxidation, Appl. Catal. B 70 (2007) 370–376.
[9] P. Harriott, J.M. Markussen, Kinetics of sorbent regeneration in the copper oxide process for flue gas cleanup, Ind. Eng. Chem. Res. 31 (1992) 373–379.
[10] C.M. Hung, Activity of Cu-activated carbon fiber catalyst in wet oxidation of ammonia solution, J. Hazard. Mater. 166 (2009) 1314–1320.
[11] P. Davini, The effect of certain metallic derivatives on the adsorption of sulphur dioxide on active carbon, Carbon 39 (2001) 419–424.
[12] H.H. Tseng, M.Y. Wey, Study of SO_2 adsorption and thermal regeneration over activated carbon-supported copper oxide catalysts, Carbon 42 (2004) 2269–2278.
[13] M.Y. Wey, C.H. Fu, H.H. Tseng, K.H. Chen, Catalytic oxidization of SO_2 from incineration flue gas over bimetallic Cu–Ce catalysts supported on pre-oxidized activated carbon, Fuel 82 (2003) 2285–2290.
[14] H.H. Tseng, M.Y. Wey, C.H. Fu, Carbon materials as catalyst supports for SO_2 oxidation: catalytic activity of CuO–AC, Carbon 41 (2003) 139–149.
[15] H.H. Tseng, M.Y. Wey, Y.S. Liang, K.H. Chen, Catalytic removal of SO_2, NO and HCl from incineration flue gas over activated carbon-supported metal oxides, Carbon 41 (2003) 1079–1085.
[16] H.H. Tseng, M.Y. Wey, Effects of acid treatments of activated carbon on its physiochemical structure as a support for copper oxide in $DeSO_2$ reaction catalysts, Chemosphere 62 (2006) 756–766.
[17] I. Mochida, Y. Korai, M. Shirahama, S. Kawano, T. Hada, Y. Seo, M. Yoshikawa, A. Yasutake, Removal of SO_2 and NO over activated carbon fibers, Carbon 38 (2000) 227–235.
[18] P. Davini, Desulphurization properties of active carbons obtained from petroleum pitch pyrolysis, Carbon 37 (1999) 1363–1371.
[19] A. Lisovskii, R. Semiat, C. Aharoni, Adsorption of sulfur dioxide by active carbon treated by nitric acid: I. Effect of the treatment on adsorption of SO_2 and extractability of the acid formed, Carbon 35 (1997) 1369–1389.
[20] A.A. Lizzio, J.A. DeBarr, Effect of surface area and chemisorbed oxygen on the SO_2 adsorption capacity of activated char, Fuel 75 (1996) 1515–1522.
[21] S. Heidenreich, M. Nacken, M. Hackel, G. Schaub, Catalytic filter elements for combined particle separation and nitrogen oxides removal from gas streams, Powder Technol. 180 (2008) 86–90.
[22] D. Fino, N. Russo, G. Saracco, V. Specchia, A multifunctional filter for the simultaneous removal of fly-ash and NO_x from incinerator flue gases, Chem. Eng. Sci. 59 (2004) 5329–5336.
[23] B. Shemwell, A. Atal, Y.A. Levendis, J.A. Simons, A laboratory investigation on combined in-furnace sorbent injection and hot flue-gas filtration to simultaneously capture SO_2, NO_x, HCl and particulate emissions, Environ. Sci. Technol. 34 (2000) 4855–4866.
[24] O. Faltsi-Saravelou, I.A. Vasalos, Simulation of a dry fluidized bed process for SO_2 removal from flue gases, Ind. Eng. Chem. Res. 29 (1990) 251–258.
[25] J. Abbasian, K.K. Ho, Development of sorbents for a fluid-bed process to control SO_x and NO_x. Final Technical Report to the Illinois Clean Coal Institute, November 1, 2000 to October 31, 2001.
[26] W.C. Yang, T.C. Ho, Handbook of Fluidization and Fluid-Particle Systems, Marcel Dekker, Inc., New York, 2003.
[27] T.C. Ho, N. Kobayashi, Y.K. Lee, C.J. Lin, J.R. Hopper, Modeling of mercury sorption by activated carbon in a confined, a semi-fluidized, and a fluidized bed, Waste Manage. 22 (2002) 391–398.
[28] J.Y. Rau, J.C. Chen, M.Y. Wey, M.D. Lin, Effects of H_2O and particles on the simultaneous removal of SO_2 and fly ash using a fluidized-bed sorbent/catalyst reactor, Ind. Eng. Chem. Res. 48 (2009) 10541–10550.
[29] J.C. Bai, S.Y. Wu, A.S. Lee, C.Y. Chu, Filtration of dust in a circulating granular bed filter with conical louver plates (CGBF-CLPs), J. Hazard. Mater. 142 (2007) 324–331.
[30] B.C. Chiang, M.Y. Wey, C.L. Yeh, Control of acid gases using a fluidized bed adsorber, J. Hazard. Mater. 101 (2003) 259–272.
[31] J.S. Klingspor, J.L. Vernon, Particulate Control for Coal Combustion, IEA Coal Res, Report IEACR/03, London, 1988.
[32] R. Zevenhoven, K. Heiskanen, Particle Technology for Thermal Power Engineers. Course material ENE-47.200, Helsinki University of Technology, Espoo, Finland, 2000, pp. 6–8.
[33] Powder Diffraction File, Joint Committee on Powder Diffraction Standards, ASTM, Philadelphia, PA, 1996 (Card 04-0836).
[34] Powder Diffraction File, Joint Committee on Powder Diffraction Standards, ASTM, Philadelphia, PA, 1996 (Card 05-0661).
[35] C.Y. Lu, M.Y. Wey, L.I. Chen, Application of polyol process to prepare AC-supported nanocatalyst for VOC oxidation, Appl. Catal. A 325 (2007) 163–174.
[36] Y. Xue, G. Lu, Y. Guo, Y. Guo, Y. Wang, Z. Zhang, Effect of pretreatment method of activated carbon on the catalytic reduction of NO by carbon over CuO, Appl. Catal. B 79 (2008) 262–269.